EPJ Web of Conferences **158**, 03001 (2017) DOI: 10.1051/epjconf/201715803001
*QFTHEP 2017*

# Rare radiative leptonic B-decays as a tool to study New Physics

*Anastasiia* Kozachuk[1,2,⋆]

[1] *Faculty of Physics, M.V. Lomonosov Moscow State University, Leninskie gory 1(2), 119991 Moscow, Russia*
[2] *D. V. Skobeltsyn Institute of Nuclear Physics, M. V. Lomonosov Moscow State University, Leninskie gory 1(2), 119991 Moscow, Russia*

**Abstract.** We present results for rare radiative leptonic B-decays $\bar{B}_{d,s} \to \gamma\ell^+\ell^-$. We calculate non-perturbative QCD part via relativistic quark model, which is a dispersion approach based on the constituent quark picture. We include the long-distance contribution, represented by light and $c\bar{c}$ vector resonances, as an additional effective term to the Wilson coefficient $C_9$. We give predictions for the branching ratios, as well as distributions of the differential rates and the forward-backward asymmetry. Finally, we consider experimental limits on the Wilson coefficient $C_{7\gamma}$ and the corresponding sensitivity of the zero-point of the forward-backward asymmetry.

## Introduction

Rare radiative leptonic B-decays proceed through flavor-changing neutral currents (FCNCs), which are forbidden at tree level in the Standard Model (SM). These currents are represented by penguin and box diagrams, which are loop diagrams, and thus lead to small probabilities of the considered decays. Because of possible contribution of new particles to the loops these decays are believed to be sensitive to physics beyond the Standard Model. There are several discrepancies between the predictions of the Standard Model and the experimental results in this sector of FCNC $b \to \{d, s\}$ transitions, which are widely discussed [1]. A well-known one is the quantity

$$\mathcal{R}_K = \frac{\mathcal{B}(B^+ \to K^+\mu^+\mu^-)}{\mathcal{B}(B^+ \to K^+e^+e^-)} = 0.745^{+0.090}_{-0.074}\,(\text{stat}) \pm 0.036\,(\text{syst})$$

in the region $q^2 \in [1;\, 6]\,\text{GeV}^2$, $q^2$ being the squared invariant mass of the lepton pair [2]. This differs from unity (the SM prediction) at $2.6\,\sigma$. A separate analysis of both of the modes showed that the deviation is rather in muons than in electrons. Another deviation comes from similar decays into $K^{*0}$ mesons:

$$\mathcal{R}_{K^{*0}} = \frac{\mathcal{B}(B^0 \to K^{*0}\mu^+\mu^-)}{\mathcal{B}(B^0 \to K^{*0}e^+e^-)} = 0.69^{+0.11}_{-0.07}\,(\text{stat}) \pm 0.05\,(\text{syst}),$$

for the region $q^2 \in [1.1;\, 6]\,\text{GeV}^2$ [3]. This gives a deviation of $2.5\,\sigma$.

Similar situation is observed for $B \to \phi\ell^+\ell^-$ decays [4]. On the other hand, the famous result for $\mathcal{B}(B_s^0 \to \mu^+\mu^-)$ obtained by LHCb and CMS is in agreement with the SM at $1\,\sigma$ level [5].

⋆e-mail: anastasiia.kozachuk@cern.ch

In this work we give theoretical predictions for rare decays $\bar{B}_{d,s} \to \gamma\ell^+\ell^-$ in the framework of the Standard Model. In Sections 1 and 2 we consider the effective Hamiltonian and the diagrams contributing to the decays. In Section 3 we discuss our calculations of the form factors within the framework of relativistic quark model. Section 4 represents our numerical results. In Section 5 we consider experimental limits of the Wilson coefficient $C_7$ and how they effect the zero-point of the forward-backward asymmetry. Section 6 is our conclusions.

## 1 Effective Hamiltonian

On the quark level rare decays $\bar{B}_{d,s} \to \gamma\ell^+\ell^-$ correspond to FCNC $b \to q$, $q = \{d, s\}$ transitions. The latter are described by an effective Hamiltonian - the Wilson operator expansion at the scale $\mu \approx 5\,\text{GeV}$, which is relevant for B-mesons[1] [6]

$$H_{\text{eff}}^{b\to q} = \frac{G_F}{\sqrt{2}} V_{tq}^* V_{tb} \sum_i C_i(\mu) O_i^{b\to q}(\mu), \tag{1}$$

here $G_F$ being the Fermi constant, $C_i$ being the Wilson coefficients and $O_i$ being the operators of the expansion. Wilson coefficients contain the contributions of massive virtual particles, such as $W$ and $Z$ bosons, and $t$-quarks. These heavy degrees of freedom, which contribute to the loop FCNC diagrams (e.g. to mentioned earlier penguin and box diagrams) are integrated out and become encoded in the Wilson coefficients. Lighter virtual particles, such as $u$ and $c$ quarks also contribute to the loop diagrams and should be taken into account separately as an addition to the effective Hamiltonian. $O_i$ are four-fermion operators which only include light quarks and leptons.

## 2 Contributions to the amplitude of $\bar{B}_{d,s} \to \gamma\ell^+\ell^-$ decays

In this section, we consider the contributions to the $\bar{B}_{d,s} \to \gamma\ell^+\ell^-$ amplitude induced by the effective Hamiltonian (1). The transition form factors are defined as follows [8, 9]:

$$\begin{aligned}
\langle\gamma^*(k,\,\epsilon)|\bar{s}\gamma_\mu\gamma_5 b|B_s(p)\rangle &= i\,e\,\epsilon_\alpha^*\left(g_{\mu\alpha}\,k'k - k'_\alpha k_\mu\right)\frac{F_A(k'^2,k^2)}{M_{B_s}},\\
\langle\gamma^*(k,\,\epsilon)|\bar{s}\gamma_\mu b|B_s(p)\rangle &= e\,\epsilon_\alpha^*\,\epsilon_{\mu\alpha k' k}\frac{F_V(k'^2,k^2)}{M_{B_s}},\\
\langle\gamma^*(k,\,\epsilon)|\bar{s}\sigma_{\mu\nu}\gamma_5 b|B_s(p)\rangle\,k'^\nu &= e\,\epsilon_\alpha^*\left(g_{\mu\alpha}\,k'k - k'_\alpha k_\mu\right)F_{TA}(k'^2,k^2),\\
\langle\gamma^*(k,\,\epsilon)|\bar{s}\sigma_{\mu\nu} b|B_s(p)\rangle\,k'^\nu &= i\,e\,\epsilon_\alpha^*\epsilon_{\mu\alpha k' k}F_{TV}(k'^2,k^2).
\end{aligned} \tag{2}$$

We define the form factors as functions of two variables, $F_i(k'^2, k^2)$, where $k'$ is the momentum emitted from the FCNC $b \to q$ vertex, and $k$ is the momentum of the photon emitted from the valence quark of the $B$-meson.

### 2.1 Lepton pair couples to the effective $b \to q$ vertex

We define $A_{(1)}^{B\to\gamma\ell\ell}$ as the contribution to the $\bar{B}_{d,s} \to \gamma\ell^+\ell^-$ amplitude, when the lepton pair is produced from the FCNC $b \to q$ vertex, while the photon is emitted from the valence quark of the $B$-meson.

[1] Our notations and conventions are: $\gamma^5 = i\gamma^0\gamma^1\gamma^2\gamma^3$, $\sigma_{\mu\nu} = \frac{i}{2}[\gamma_\mu, \gamma_\nu]$, $\varepsilon^{0123} = -1$, $\epsilon_{abcd} \equiv \epsilon_{\alpha\beta\mu\nu}a^\alpha b^\beta c^\mu d^\nu$, $e = \sqrt{4\pi\alpha_{\text{em}}}$.

Diagrams, contributing to $A_{(1)}^{B\to\gamma\ell\ell}$ are shown in Figure 1. In this case we denote the momenta as $k' = q$, $k = p - q$, $k'^2 = q^2$ and $k^2 = 0$, thus obtaining $F_i(q^2, 0)$:

$$A_{(1)}^{B\to\gamma\ell\ell} = \langle\gamma(k,\,\epsilon),\,\ell^+(p_1),\,\ell^-(p_2)|H_{\rm eff}^{b\to d\ell^+\ell^-}|B(p)\rangle \;=\; \frac{G_F}{\sqrt{2}}\,V_{tb}V_{tq}^*\,\frac{\alpha_{\rm em}}{2\pi}\,e\,\epsilon_\alpha^* \tag{3}$$

$$\times\Big[\epsilon_{\mu\alpha k'k}A_V^{(1)}(q^2)\bar\ell(p_2)\gamma_\mu\ell(-p_1) - i\left(g_{\mu\alpha}\,k'k \;-\; k'_\alpha k_\mu\right)A_A^{(1)}(q^2)\bar\ell(p_2)\gamma_\mu\ell(-p_1)$$

$$+\epsilon_{\mu\alpha k'k}A_{5V}^{(1)}(q^2)\bar\ell(p_2)\gamma_\mu\gamma_5\ell(-p_1) - i\left(g_{\mu\alpha}\,k'k \;-\; k'_\alpha k_\mu\right)A_{5A}^{(1)}(q^2)\bar\ell(p_2)\gamma_\mu\gamma_5\ell(-p_1)\Big], \tag{4}$$

$k' = q$, $k = p - q$ and

$$A_{V(A)}^{(1)}(q^2) = \frac{2m_b\,C_{7\gamma}(\mu)}{q^2}F_{TV(TA)}(q^2,0) + C_{9V}(\mu)\frac{F_{V(A)}(q^2,0)}{M_B}, \tag{5}$$

$$A_{5V(5A)}^{(1)}(q^2) = C_{10AV}(\mu)\frac{F_{V(A)}(q^2,0)}{M_B}. \tag{6}$$

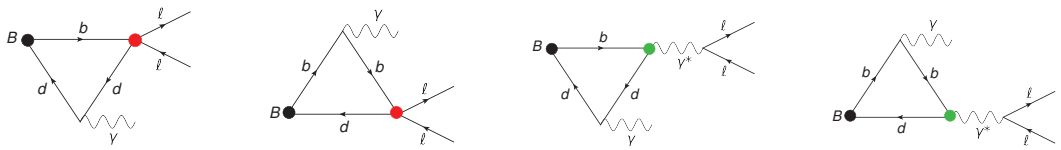


**Figure 1.** Diagrams, contributing to $A_{(1)}^{B\to\gamma\ell\ell}$ amplitude

### 2.2 Effective $b \to q$ vertex emits a real photon

Another contribution to the amplitude, which we denote as $A_{(2)}^{B\to\gamma\ell\ell}$, is relevant for the process when the real photon is emitted from the penguin FCNC vertex, while the valence quark of the $B$-meson emits a virtual photon.The diagrams, contributing to $A_{(2)}^{B\to\gamma\ell\ell}$ are shown on Figure 2.2.

The amplitude $A_{(2)}^{B\to\gamma\ell\ell}$ has the same Lorentz structure as the $C_{7\gamma}$ part of $A^{(1)}$ but now the momenta are defined as $k = q$, $k' = p - q$, $k'^2 = 0$ and $k^2 = q^2$. The amplitude thus includes the form factors $F_{TA,TV}(0, q^2)$, with $F_{TA}(0, q^2) = F_{TV}(0, q^2)$:

$$A_{(2)}^{B\to\gamma\ell\ell} \;=\; \frac{G_F}{\sqrt{2}}\,V_{tb}V_{tq}^*\,\frac{\alpha_{\rm em}}{2\pi}\,e\,\epsilon_\mu^*\bar\ell(p_2)\gamma_\alpha\ell(-p_1) \tag{7}$$

$$\times\;\;\Big[\varepsilon_{\mu\alpha k'k}A_V^{(2)}(q^2) - i\left(g_{\mu\alpha}k'k - k'_\alpha k_\mu\right)A_A^{(2)}(q^2)\Big],\quad k = q,\quad k' = p - q,$$

where

$$A_{V(A)}^{(2)}(q^2) = \frac{2m_bC_{7\gamma}(\mu)}{q^2}F_{TV(TA)}(0,q^2). \tag{8}$$

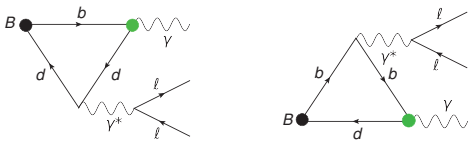


**Figure 2.** Diagrams, contributing to $A_{(2)}^{B\to\gamma\ell\ell}$ amplitude

In addition to the amplitudes described in Sections 2.1 and 2.2 we also include the contribution of bremsstrahlung and weak annihilation. We do not discuss the details here in order not to overload this paper.

## 3 Parametrization for the $F_i$ form factors

In this section we discuss the parametrization for the form factors defined in (2).

### 3.1 Form factors $F_i(q^2, 0)$

We calculate the form factors $F_i(q^2, 0)$ in the framework of relativistic quark model which is a dispersion approach based on the constituent quark picture [7]. Each form factor is represented as a dispersion integral over the mass variable. The integrand in each case is a complicated function, for some details of the calculation see, for e.g. [10]. In case of radiative leptonic decays $\bar{B}_{d,s} \to \gamma\ell^+\ell^-$ we obtain form factors as functions of $q^2$, where $q^2$ is the squared invariant mass of the lepton pair. It is convenient to introduce every form factor as a sum of two parts

$$F_i(q^2) = Q_b F^{(b)}(q^2)_i + Q_{d,s} F^{(d,s)}(q^2). \tag{9}$$

Finally, we use the following parametrization:

$$F_i^{(\alpha)}(q^2) = \frac{F_i^{(\alpha)}(0)}{1 - q^2/M_{R_i}^2}, \tag{10}$$

where the parameters $F_i^{(\alpha)}(0)$ and $M_{R_i}$ are presented in Tables 1 and 2.

**Table 1.** Parameters $F_i^{(\alpha)}(0)$ and $M_{R_i}$ for the $\bar{B} \to \gamma\ell\ell$ form factors

| | $F_V^{(d)}$ | $F_V^{(b)}$ | $F_A^{(d)}$ | $F_A^{(b)}$ | $F_{TV}^{(d)}$ | $F_{TV}^{(b)}$ | $F_{TA}^{(d)}$ | $F_{TA}^{(b)}$ |
|---|---|---|---|---|---|---|---|---|
| $F(0)$ | -0.295 | -0.037 | 0.259 | 0.042 | -0.313 | -0.04 | -0.313 | -0.04 |
| $M_R$ | 5.6 | 5.55 | 5.9 | 5.45 | 5.6 | 5.6 | 6.0 | 6.2 |

**Table 2.** Parameters $F_i^{\alpha}(0)$ and $M_{R_i}$ for the $\bar{B}_s \to \gamma\ell\ell$ form factors

| | $F_V^{(s)}$ | $F_V^{(b)}$ | $F_A^{(s)}$ | $F_A^{(b)}$ | $F_{TV}^{(s)}$ | $F_{TV}^{(b)}$ | $F_{TA}^{(s)}$ | $F_{TA}^{(b)}$ |
|---|---|---|---|---|---|---|---|---|
| $F(0)$ | -0.289 | -0.043 | 0.257 | 0.049 | -0.305 | -0.046 | -0.305 | -0.046 |
| $M_R$ | 5.6 | 5.6 | 5.9 | 5.5 | 5.6 | 5.6 | 6.0 | 6.2 |

### 3.2 Form factors $F_i(0, q^2)$

For the form factors $F_{TV,TA}(0, q^2)$ we use the VMD formula, which includes decay constants $f_V$ of light vector resonances and $B \to V$ transition form factors:

$$F_{TV,TA}(0, q^2) = F_{TV,TA}(0, 0) - \sum_V 2 f_V^{\text{e.m.}} g_+^{B\to V}(0) \frac{q^2/M_V}{q^2 - M_V^2 + iM_V\Gamma_V}, \tag{11}$$

where $M_V$ and $\Gamma_V$ are the mass and the width of the vector meson resonance, $g_+^{B\to V}(0)$ are the $B \to V$ transition form factors, defined according to the relations

$$\langle V(q,\varepsilon)|\bar{d}\sigma_{\mu\nu}b|B(p)\rangle = i\varepsilon^{*\alpha}\epsilon_{\mu\nu\beta\gamma}\left[g_+^{B\to V}(k^2)g_{\alpha\beta}(p+q)^\gamma + g_-^{B\to V}(k^2)g_{\alpha\beta}k^\gamma + g_0^{B\to V}(k^2)p_\alpha p^\beta q^\gamma\right].$$

The form factors $g_+^{B\to V}(0)$ were calculated via relativistic quark model in [7]. The e.m. leptonic decay constant of a vector meson is given by

$$\langle 0|j_\mu^{\text{e.m}}|V(\varepsilon,p)\rangle = \varepsilon_\mu M_V f_V^{\text{e.m.}}. \tag{12}$$

**Table 3.** Values of the mass and the width of neutral vector mesons [12], decay constant $f_V$ (with isotopic factors omitted) extracted from the leptonic width neglecting the meson-mixing effects, and the $g_+^{B\to V}(0)$ calculated via dispersion quark model.

| V | $M_V$, MeV | $\Gamma_V$, MeV | $f_V$, MeV | $g_+^{B\to V}(0)$, GeV |
|---|---|---|---|---|
| $\rho^0$ | 775 | 149 | 220 | 0.29 |
| $\omega$ | 783 | 8.49 | 195 | 0.24 |
| $\phi$ | 1019 | 4.27 | 226 | 0.27 |

The electromagnetic decay constants which enter the VMD formula (11) are related to $f_V$ as follows: $f_{\rho^0}^{\text{e.m.}} = \frac{1}{\sqrt{2}} f_{\rho^0}$, $f_\omega^{\text{e.m.}} = \frac{1}{3\sqrt{2}} f_\omega$, $f_\phi^{\text{e.m.}} = -\frac{1}{3} f_\phi$.

## 4 Numerical Results

In this section we present our numerical results for the decays $\bar{B}_{d,s} \to \gamma l^+ l^-$. We give two estimates for the branching ratios: the first one for the range $q^2 \in [1;6]\,\text{GeV}^2$, which does not include any resonances, and the second one for the whole range of the invariant mass of the lepton pair. We include the long-distance contribution, represented by light and $c\bar{c}$ vector resonances, using a simple Breit-Wigner formula [11]. The numerical predictions are given in Table 4. In Figure 3 we present out results for the distributions of the differential branching ratios and the forward-backward asymmetry for $\bar{B}_{d,s} \to \mu^+\mu^-\gamma$ decays.

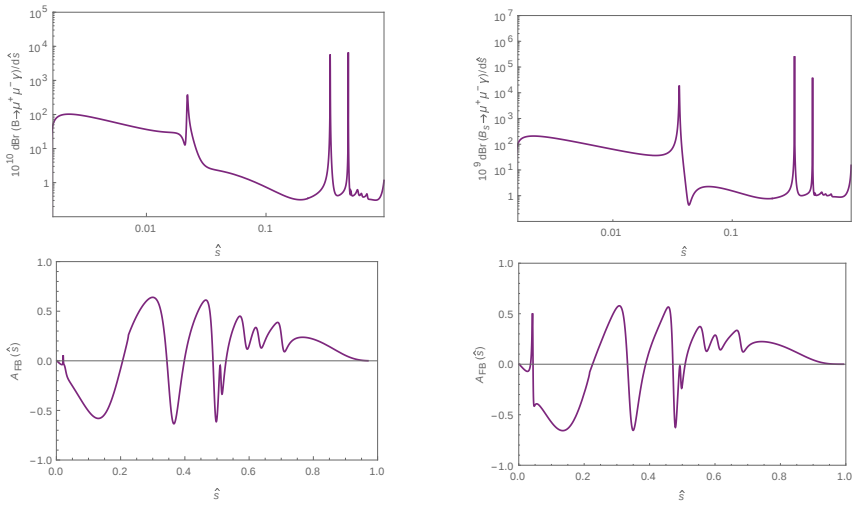


**Figure 3.** Differential branching ratios and forward-backward asymmetries for $\bar{B}_d \to \gamma\mu^+\mu^-$ (left) and $\bar{B}_s \to \gamma\mu^+\mu^-$ (right) decays, $\hat{s} = q^2/M_B^2$

**Table 4.** Our results for the branching ratios of $\bar{B}_{d,s} \to l^+ l^- \gamma$ decays for different ranges of $q^2$: for $q^2 \in [1;6]\,\mathrm{GeV}^2$ and for the full range. The value of the photon energy cut is 500 MeV

| $q^2$-range | $[1;6]\,\mathrm{GeV}^2$ | Full |
|---|---|---|
| $Br(B \to e^+e^-\gamma) \times 10^{10}$ | 0.12 | 4.6 |
| $Br(B \to \mu^+\mu^-\gamma) \times 10^{10}$ | 0.12 | 1.5 |
| $Br(B_s \to e^+e^-\gamma) \times 10^{9}$ | 0.76 | 18.4 |
| $Br(B_s \to \mu^+\mu^-\gamma) \times 10^{9}$ | 0.73 | 11.6 |

## 5 Experimental limits on $C_7$ and the forward-backward asymmetry

After obtaining results within the Standard Model, we started to look at different possibilities of including the effects of New Physics into our calculations. One of the simplest opportunities was to try to change the values of the Wilson coefficients within available experimental limits and to look at the corresponding sensitivity of the observables. So far we implemented this idea in comparing the distributions of the forward-backward asymmetry for different values of the Wilson coefficient $C_{7\gamma}$. We expect the forward-backward asymmetry to be almost independent from the model of the form factors description and thus sensitive to possible NP effects. In Figure 4 [13] one can see all the range of possible values for NP contributions to the Wilson coefficient $C_{7\gamma}$ (we assume that $C_{7\gamma} = C_{7\gamma}^{SM} + C_{7\gamma}^{NP}$).

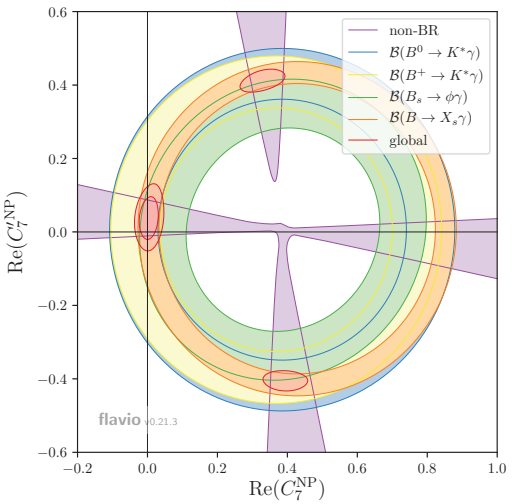


**Figure 4.** $C_7 - C_7'$ plot: experimental limits [13]

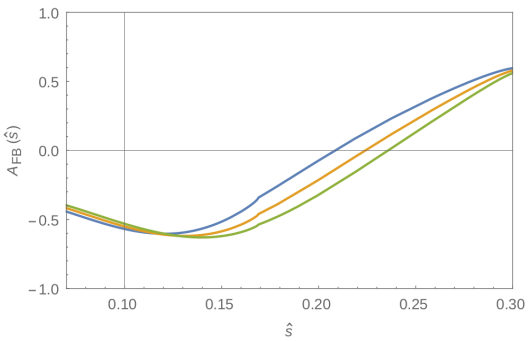


**Figure 5.** Sensitivity of the zero-point of the forward-backward asymmetry to the change of $C_{7\gamma}$ Wilson coefficient within its experimental limits, $\hat{s} = q^2/M_B^2$

We have plotted the forward-backward asymmetry for three of possible values of $C_{7\gamma}$: 0.276, 0.308 and 0.335 (see Figure 5). This range of values correspond to the case $C_7' = 0$, which is in agreement with our calculations. One can see that such a small change of $C_{7\gamma}$ has almost no impact on the position of the zero-point of the forward-backward asymmetry.

## 6 Conclusions

We gave predictions for rare radiative leptonic decays $\bar{B}_{d,s} \to \gamma\ell^+\ell^-$. We calculated the form factors $F_i(q^2, 0)$ via relativistic quark model. Form factors $F_i(0, q^2)$ were taken into account via vector meson dominance. We included the long-distance contribution: light and $c\bar{c}$ vector resonances via simple Breit-Wigner formula. We obtained numerical predictions for the branching ratios and distributions for the branching fractions and the forward backward asymmetry. We found very small sensitivity of the zero-point of the forward-backward asymmetry to the change of the Wilson coefficient $C_{7\gamma}$ within its experimental limits. We are now working on a better way of including the $c\bar{c}$-resonances and the continuum above the $D\bar{D}$-threshold.

## Acknowledgments

The author would like to thank Diego Guadagnoli, Dmitri Melikhov, Nikolai Nikitin and Peter Strangl for useful discussions. The work was supported by grant RNF-16-12-10280 of the Russian Science Foundation.

## References

[1] D. Guadagnoli, D. Melikhov and M. Reboud, Phys. Lett. B **760**, 442 (2016)
[2] LHCb Collaboration, Phys. Rev. Lett. **113**, 151601 (2014)
[3] LHCb Collaboration, JHEP **08**, 055 (2017)
[4] LHCb Collaboration, JHEP **09**, 179 (2015)
[5] CMS and LHCb Collaborations, Nature **522**, 68 (2015)
[6] B. Grinstein, M. J. Savage and M. B. Wise, Nucl. Phys. B **319**, 271 (1989)
[7] D. Melikhov, Phys. Rev. D **53**, 2460 (1996); D. Melikhov, Phys. Rev. D **56**, 7089 (1997)
[8] F. Kruger and D. Melikhov, Phys. Rev. D **67**, 034002 (2003)
[9] D. Melikhov and N. Nikitin, Phys. Rev. D **70**, 114028 (2004)
[10] A. Kozachuk, D. Melikhov and N. Nikitin, Phys. Rev. D **93**, 014015 (2016)
[11] A. Ali, T. Mannel and T. Morozumi, Phys. Lett. B **273**, 505 (1991)

[12] Particle Data Group, Chin. Phys. C **40**, 100001 (2016)
[13] A. Paul and D. M. Straub, JHEP **1704**, 027 (2017); P. Strangl, "Constraints on the Wilson coefficients C7 and C7" ' June, 2017, https://doi.org/10.5281/zenodo.804453